



In Silico Analysis of *Calotropis procera*-Derived Phytochemicals Targeting 3CL Protease of SARS-CoV-2

Tayyaba Shafique¹ · Mohsin Javed¹ · Muhammad Ali² · Shahid Iqbal³ · Muhammad Faizan⁴ · Ammar Zidan⁵ · Ali Bahadur^{6,7} · Sajid Mahmood^{3,8} · Fadi Jaber^{9,10} · Khalid M. Alotaibi¹¹ · Matar Alshawi¹¹

Received: 17 November 2023 / Accepted: 15 July 2024

© The Author(s), under exclusive licence to Springer Science+Business Media, LLC, part of Springer Nature 2024

Abstract

The coronavirus known as SARS-CoV-2 has enveloped virions with single-stranded positive-sense RNA genome. It infects mammals, including humans, via the respiratory tract. The non-structural protein of coronavirus, main protease (3CLp) is a key enzyme in the disease's progression. This study aimed to screen phytochemicals derived from *Calotropis Procera* as potential drugs against 3CLp. Through database search, 50 phytochemicals were identified in the *Calotropis* sp. To evaluate the possible drug-like properties of these phytochemicals, the studies like, ADMET (Absorption, Distribution, Metabolism, Excretion, Toxicity) analysis, molecular docking and density functional theory (DFT) were performed. Furthermore, GC–MS was performed using water and ethanolic extracts from the plant leaves. The ADMET analysis and docking results showed 11 phytochemicals as probable drug candidates against 3CLp of SARS-CoV-2. All these phytochemicals showed ≥ -4.3 kcal/mol binding affinity, similar to previously reported inhibitors. Furthermore, based on band energy gap, EHOMO, ELUMO, and DFT analyses, it was shown that these phytochemicals had a significant level of reactivity necessary for the interaction. Among all, the phytochemicals uscharin, voruscharin, frugoside, coroglaucigenin, and benzoylisolineolone may be considered the top 5 drug-like candidates against 3CLp. Furthermore, the selected phytochemicals may be employed for in vitro and in vivo studies for the advancement of a probable drug alongside SARS-CoV-2.

Keywords ADMET · Antivirus · COVID-19 · DFT · Medicinal plants · Molecular docking

✉ Shahid Iqbal
shahidiqbal@hzu.edu.cn

✉ Ali Bahadur
abahadur@wku.edu.cn

✉ Sajid Mahmood
sajidmahmood1987@yahoo.com

¹ Department of Chemistry, School of Science, University of Management and Technology, Lahore 54770, Pakistan

² Department of Biochemistry, School of Sciences, University of Management and Technology, Lahore 54770, Pakistan

³ Nottingham Ningbo China Beacons of Excellence Research and Innovation Institute, University of Nottingham Ningbo China, Ningbo 315100, China

⁴ Department of Chemical and Material Engineering, Chang Gung University, Taoyuan, Taiwan

⁵ Biomedical Engineering Department, College of Engineering and Technologies, Al-Mustaqbal University, 51001 Babylon, Iraq

⁶ Nanomaterials Research Center, Department of Chemistry, College of Science, Mathematics, and Technology, Wenzhou-Kean University, Wenzhou 325060, Zhejiang Province, China

⁷ Dorothy and George Hennings College of Science, Mathematics and Technology, Kean University, 1000 Morris Ave, Union, NJ 07083, USA

⁸ Functional Materials Group, Gulf University for Science and Technology, 32093 Mishref, Kuwait

⁹ Department of Biomedical Engineering, Ajman University, Ajman, UAE

¹⁰ Center of Medical and Bio-Allied Health Sciences Research, Ajman University, Ajman, UAE

¹¹ Department of Chemistry, College of Science, King Saud University, PO Box 2455, 11541 Riyadh, Saudi Arabia

Introduction

Viruses are made up of hereditary material that is encased in a protein coat. They can cause diseases as severe as HIV/AIDS and CoVID-19 (Coronavirus disease 2019) [1]. Viral infections are currently regarded as a public health issue. The current COVID-19 pandemic is triggered by the Coronavirus-2 linked with severe acute respiratory syndrome (SARS-CoV-2). Coronaviruses (CoVs) are associates of the *Coronaviridae* family of order *Nidovirales* [2, 3]. Coronaviruses are classified into four sub-groups known as alpha, beta, gamma, and delta [4, 5]. The crown-like spikes on their surface gave them their name. One of the seven coronaviruses that infect humans, SARS-CoV-2 is a member of the beta subgroup [6].

In 1931, the first coronavirus-based disease was identified, and the first coronavirus (HCoV-229E) was isolated from humans in 1965. Until SARS-CoV, only HCoV-229E and HCoV-OC43 were known [7]. It is a chronic and frequently fatal respiratory illness that was first recorded in November 2002 in Guangdong Province, China, with 11% mortality [8, 9]. Then, in 2012, a Middle East Respiratory Syndrome (MERS-CoV) epidemic brought on by -coronaviruses belonging to the Merbecovirus subgenus was noticed in Saudi Arabia, with a fatality rate of 34% [4, 10]. According to the World Health Organization (WHO), COVID-19 initially coarse in Wuhan (China) in December 2019. It is a contagious illness that mostly affects the respiratory system. SARS-CoV-2, a recently identified coronavirus, is the culprit [11, 12].

Large, enclosed, positive-sense, single-stranded RNA viruses called coronaviruses cause diseases by infecting the respiratory systems of animals, including humans [13–15]. Three phases characterize the progression of the COVID-19 viral infection: the asymptomatic cycle, the non-severe symptomatic phase, and the serious infection stage [16]. Spike (S), nucleocapsid (N) envelope (E), and membrane (M) are the fundamental proteins of SARS-CoV-2 [17, 18]. Via the ACE2 receptor, the S protein may engage in robust interactions with the host cell [19]. Following the attachment of the virus's S protein to the ACE2 receptor, the virus's envelope will merge with the membrane of the host cell and enter the cell [17, 20, 21].

Due to their medicinal properties, plants have long been important for human wellness [22]. The WHO estimates that about 80% of people on the planet rely on medicinal plants or herbs to take care of their medical requirements [23, 24]. To tackle this global pandemic, scientists are assessing antiviral plant secondary metabolites (PSMs) as sources of therapeutic drugs and looking for novel medical plant-derived drugs [25]. Studies have demonstrated that plant metabolites can disrupt signaling pathways within

cells, prevent the coronavirus S protein from combining with the host's ACE2, and decrease the activity of coronavirus-reproduction cycle-related enzymes such as 3CL protease and papain-like protease [26, 27]. Therefore, the goal of the current work was to use computer-assisted analysis to identify possible phytochemicals with high binding affinities from sources of medicinal plants against COVID-19.

Calotropis procera, the milkweed shrub or Sodom apple, is a flowering plant native to tropical and sub-tropical areas of the world. It is long been known in traditional medicine and is considered an important plant for treating ailments asthma, diarrhea, dysentery, leprosy, malaria, skin diseases, and snake bites. Also, there are concerns regarding its poisonous effects, like ingesting any part of the plant may be fatal. However, the phytochemicals in this plant have been shown to have inhibitory effects against several viral and bacterial diseases [28].

Since a large number of compounds are under investigation, drug screening using *in vitro* and *in vivo* analysis has become more complex, time taking, and expensive. The *in silico* approach utilizing computational techniques aid the drug invention procedure by making the investigation economical and resource-efficient. In this *in silico* analysis, phytochemicals derived from the medicinal plant *Calotropis procera*, which is locally found in South Asia, are used to analyze their interaction with the core protease (3CLp) protein of SARS-CoV-2. The present study's goal is to examine the phytochemicals obtained from *Calotropis procera*'s interaction potential with SARS-primary CoV-2's protease.

Materials and Methods

Phytochemicals from the plant *Calotropis procera* were tested for antiviral activity against SARS-CoV-2.

GC–MS Analysis

Calotropis Procera methanolic and water extracts were used to determine their composition using GC–MS. Helium was employed as a carrier gas at constant pressure. A 20:1 split ratio was used to inject the methanolic and water extract (1 μ L) into the GC. The injection temperature was set at 250 °C. The chromatogram's peak area will be used to measure the concentration of each analyte.

Selection of Phytochemicals

Dr. Duke's Phytochemical and Ethnobotanical Databases were used to search for phytochemicals in the *Calotropis Procera* plant. PubChem and Swiss ADME were used to

search canonical smiles of selected phytochemicals that were required for docking and ADMET reports.

Assessment of Phytochemicals (ADMET and Drug-likeness Prediction)

The phytochemicals were screened based on ADMET properties and drug-interaction prediction by using the Swiss ADME, Pre ADMET, and cbligand.org online servers. The phytochemicals' pharmacological properties and pharmacokinetics, such as gastrointestinal (GI) solubility (ESOL), absorption, blood–brain barrier (BBB) penetration and violations of Lipinski's rules, were investigated [29]. The criteria for screening phytochemicals are listed in Table 1.

Retrieval and Assessment of Protein Structure

We obtained the major protease protein for SARS-CoV-2 (PDB ID:6XA4, resolution 1.65) from the protein data bank (PDB; www.rcsb.org). Chimera 1.14 was used to remove the inhibitor attached to the protein's 3D structure and to find the active site of the protein. PyMol, Chimera 1.14, and the Discovery Studio Visualizer were used to check the active site. Ramachandran Plot was used to determine the reliability of the protein structure, which was done using the PROCHECK V6.0 online server [30]. ExPasy protparam server was used to perform a physiochemical analysis of virus protein. The following variables were calculated: Aliphatic 5 Index (AI), Isoelectric Point (PI), Instability Index (II), Number of Positively Charged Residues (+R), Number of Negatively Charged Residues (-R), Extinction Coefficient (EC) at 280 nm; GOR4 online service was utilized

to forecast and evaluate the secondary structure, as well as GRAVY—Grand Average of Hydrophobicity [31].

Protein–Protein Interaction (PPI)

We looked at how viral proteins interacted with human proteins as well as their roles using the VIRUSES online interface, which is part of STRING version 10.5 [32]. This server is used to predict the relationship between the SARS-CoV-2 protein (NCBI taxonomic ID: 694,009) and Homo sapiens protein (NCBI taxonomy Id: 9606).

Molecular Docking

AutoDock Vina incorporated in Chimera 1.14 was used to assess molecular docking of the SARS-CoV-2 protein 3CLp with certain phytochemicals [33, 34].

Dock Preparation and Visualization

Via canonical smiles, selected phytochemical (ligand) structures were created, minimized, and saved as mol files. By choosing the conjugate gradient steps to be set to 10, the steepest descent steps to be set to 100, the steepest descent step size of 0.02 Å, and the steepest gradient steps to be set to 10, the phytochemical structure was reduced. To consider the protonation state: of histidine and slower H-Bonds, hydrogen was added first, followed by charges. With the help of the dock prep command, the protein (receptor) structure was surface edited. The inhibitor was then removed, incomplete side chains were swapped out for those from the Dunbrack 2010 rotamer library, hydrogen and charges were added to the protein structure, and the finished file was saved

Table 1 Identification of the compounds in *Calotropis Procera*

No	Compounds	Formula	Retention time	Peak area
1	1-Octadecene	C ₁₈ H ₃₆	0.154	12.58
2	4-Methylamphetamine	C ₁₀ H ₁₅ N	1.302	26.65
3	1,2-Benzenedicarboxylic acid	C ₈ H ₆ O ₄	5.936	1.61
4	Phytol	C ₂₀ H ₄₀ O	7.157	2.68
5	Di isooctyl phthalate	C ₂₄ H ₃₈ O ₄	9.066	1.97
6	Beta caryophyllene	C ₁₅ H ₂₄	10.516	1.31
7	Cannabidivarin	C ₁₉ H ₂₆ O ₂	11.036	2.72
8	5-Cholestene-3-ol	C ₂₈ H ₄₈ O	11.682	2.34
9	Stigmasterol	C ₂₉ H ₄₈ O	11.767	2.21
10	Gamma sitosterol	C ₂₉ H ₅₂ O ₂	11.972	1.89
11	Beta Amyrin	C ₃₀ H ₅₀ O	12.315	3.47
12	Alpha Amyrin	C ₃₀ H ₅₀ O	12.329	9.16
13	Acetate	C ₂ H ₃ O ₂	12.619	4.47
14	Lupeol	C ₃₀ H ₅₀ H	12.745	3.77
15	Bolasterone	C ₂₁ H ₃₂ O ₂	13.078	9.09
16	Epinephrine	C ₉ H ₁₃ NO ₃	11.350	2.00

in the mol format. The Discovery studio visualizer was used to view the binding pockets, binding residues, and H-bonds in the 2D and 3D structures of the resulting complexes. For the visualization of 2D or 3D structures, the ligand-receptor complex file in pdb format was provided.

Density Functional Theory (DFT) Analysis

Gaussian and GaussView were used for DFT calculations [35, 36]. Transition energies of selected phytochemicals used against the main protease were measured at the ground state utilizing DFT calculations on optimized structures using B3LYP functional (3-parameter, the Becke, Lee-Yang-Parr hybrid functional) to evaluate their reactivity and proficiency [37]. The HOMO and LUMO energies were used in the study. The basis set that was selected is 6-311G (d, p, ++).

GC-MS Assessment

GC-MS assessment was conducted to evaluate the qualitative and quantitative composition of *Calotropis Procera*, and the findings are shown in Table 1 and Fig. 1. A total of 20 compounds were identified. 1-octadecene, phytol, 5-cholestene-3-ol, stigmasterol, gamma sitosterol, beta amyryn, and alpha amyryn are the main constituents. Those phytochemicals that showed the best results in molecular docking and DFT analysis were not detected in GC-MS analysis, possibly due to their inability to dissolve in methanol and water. Furthermore, the GC-MS analysis was performed using plant leaf samples, however, Dr. Duke's Phytochemical and Ethnobotanical Databases showed them to express at high level in floral parts of the plant.

Drug Likelihood Prediction

The ADMET properties and drug-likeness of all phytochemicals were assessed. The criteria mentioned in

Supplementary Table 1 were used to screen these phytochemicals. These phytochemicals were also screened using Lipinski's rule of five [38]. The molecular characteristics of substances significant to the pharmacokinetic potential of a medicine are explained by Lipinski's rule [29]. These laws are critical for a phytochemical being used as an oral medicine [39]. Phytochemicals that meet these criteria are exposed to further docking studies. A total of 14 phytochemicals out of 50 met the requirements for being drug-like and possessing appropriate ADMET profiles. Supplementary Table 2 lists the phytochemicals that were screened, and Supplementary Table 3 lists their general properties.

Quality Assessment of Protein Structure

The primary physiochemical analysis has been conducted, and the amino acid composition was determined. The main protease was observed to be made up of twenty-two amino acids of various compositions (data not shown). Leucine had the highest content of these amino acids (9.5%). It demonstrates the protein's hydrophobic nature. The length of the sequence is 306 and the molecular weight is 33.8 kDa. This protein's isoelectric point is 5.95, indicating the protein's basic nature. Positively charged residues (Arg + Lys) account for 22 of the total, while negatively charged residues (Asp + Glu) account for 26. At 280 nm, the extinction coefficient of this protein was 33,640. The effectiveness of protein-ligand or protein-protein interactions' quantification is evaluated using this value. The protein's instability index, which is 27.65, was used to evaluate the protein's stability. This value means that the protein in a test tube is unstable. The aliphatic index of a protein indicates how much of the protein is taken up by aliphatic chains (Alanine, Valine, Isoleucine, and Leucine). This protein has an aliphatic index of 82.12. The hydrophobicity of amino acid residues in a protein is measured by Grand Average Hydropathicity. The hydropathicity of this protein is - 0.019. (data not shown). This protein molecule contains 5 different atoms: C, H, N,

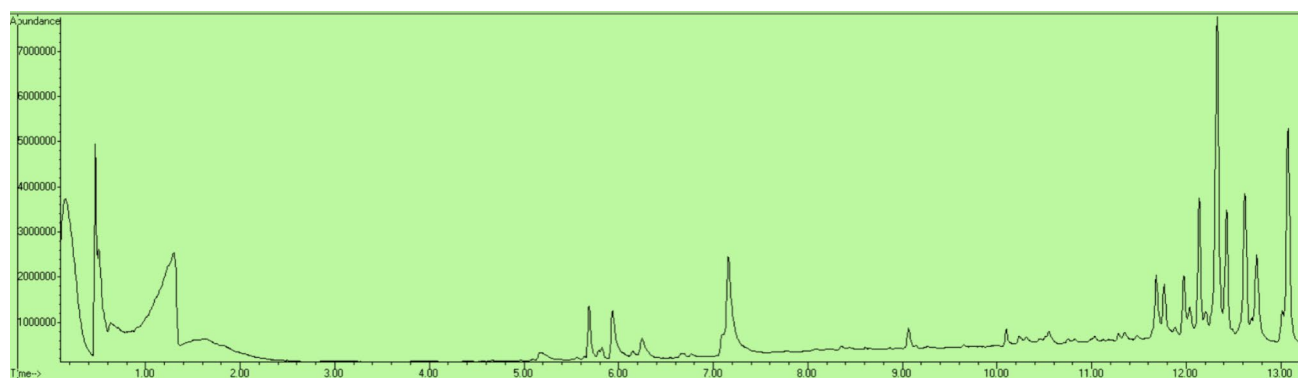


Fig. 1 GC-MS chromatogram of *Calotropis Procera* sample

O, and S, 4686 are the total number of atoms present in this protein and the molecular formula is $C_{1499}H_{2318}N_{402}O_{445}S_{22}$.

The local conformation proteins' polypeptide backbone is referred to as a protein secondary structure. β -strand (E) and α -helix (H) are the regular resulting structure states and the spiral region (C) is the irregular secondary structure state. Sander developed the DSSP (Dictionary of Secondary Structure of Proteins) secondary structure assignment system [41]. According to hydrogen-bonding patterns, it automatically divides the secondary structure into 8 conditions (H, E, B, T, S, L, G, and I). The three categories of helix, sheet, and coil are often used to categorize these eight states. Helixes are classified as G, H, and I according to the most widely used convention, sheets as B and E, and all other states as coils.

A Ramachandran plot [40] was developed to evaluate the quality of the protein structure for the major protease protein of SARS-CoV-2. Analyzing the possible angles and conformations for each individual amino acid residue in the primary protease model showed that 89.0 percent of residues were in the most preferred zone, 9.8 percent were in the additional region, 0.8 percent were in the generously allowed region, and only 0.4 percent were in the disallowed zone. The total number of residues was 304, and the properties of

the residues revealed that the maximum deviation was 5.6 and the bond length was 4.8.

Protein–Protein Interaction (PPI)

Protein–protein interactions of the viral protein 3CLp within the host cell showed its importance as a target protein. The viral protein 3CLp protein is directly linked with the human proteins CXCL10, EIF2C1, EIF2C2, EIF2C3, and EIF2C4 according to an analysis of the virus-host PPI network (Fig. 2). 3CLp and CXCL10 had a combined interaction score of 0.652, while 3CLp and EIF2C1, EIF2C2, EIF2C3, and EIF2C4 had a combined interaction score of 0.584 (Table 2), suggesting a close relationship. Table 3 summarizes the functions of human protein receptors that interact with virus protein.

Molecular Docking Studies

The 3CL^{Pro} is previously been explored extensively in the recent era [42], however, further research is necessary to explore full inhibitory potential. In our study 14 chosen phytochemicals' binding scores to the target protein were utilized to calculate binding energy and inhibitory constant

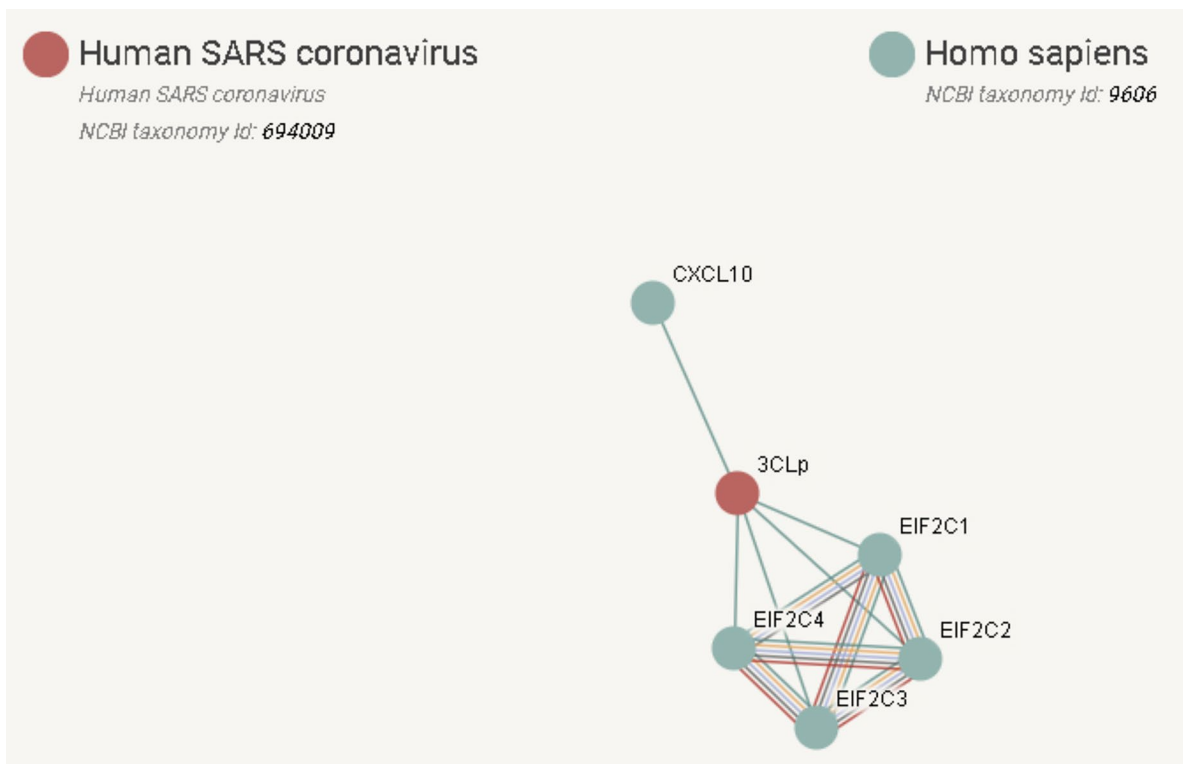


Fig. 2 A virus-human protein–protein interaction (PPI) network shows the connections between the human SARS coronavirus and Homo sapiens proteins. The viral proteins are represented by red circles, while the human proteins are represented by gray circles. The

type of interaction is indicated by the color of the lines (edges), the thickness of the edges demonstrates the intensity of the supporting data, and the number of interactions is shown by the different edges of different colors

Table 2 Virus-Host protein–protein interaction score

Virus protein	Human Receptor	Interaction Score
33C like proteinase (3CLp)	CXCL10	0.652
	EIF2C1	0.584
	EIF2C2	0.584
	EIF2C3	0.584
	EIF2C3	0.584

(K_i) values. The ligand-receptor complexes were chosen using a -4.3 kcal/mol threshold. A total of 11 phytochemicals had a binding attraction of ≥ -4.3 kcal/mol, indicating their use as potential drugs against 3CLp.

Uscharin has a binding attraction of -6.7 kcal/mol, which is the greatest, and two hydrogen bonds. Voruscharin forms two hydrogen bonds and has a binding affinity of -6.5 kcal/mol. The binding affinity of coroglaucigenin is -5.6 kcal/mol with a single hydrogen bond. The binding affinity of fructoside, which contains two hydrogen bonds, is -5.4 kcal/mol. With a binding affinity of -5.1 kcal/mol, benzoylisolineolone attaches to two hydrogen bonds. The binding affinity of uzarigenin is -5.0 kcal/mol, and it only binds to one hydrogen bond. Corotoxigenin has a -4.9 kcal/mol binding affinity with two hydrogen bonds. Isolineolone has a binding affinity with one hydrogen bond of -4.9 kcal/mol. The binding affinity of caloropagenin is -4.8 kcal/mol and it binds to two hydrogen bonds. The

binding affinity of syriogenin is -4.8 kcal/mol and it only binds to one hydrogen bond. Lineolone has a -4.4 kcal/mol binding affinity with two hydrogen bonds. A three-dimensional representation of phytochemicals in the binding pocket of the primary protease crystal structure is shown in Fig. 3. Docking results depict that uscharin forms the strongest interactions. Table 4 summarizes 2D representations of ligand-receptor complexes, along with their interacting amino acids, binding scores, and K_i values.

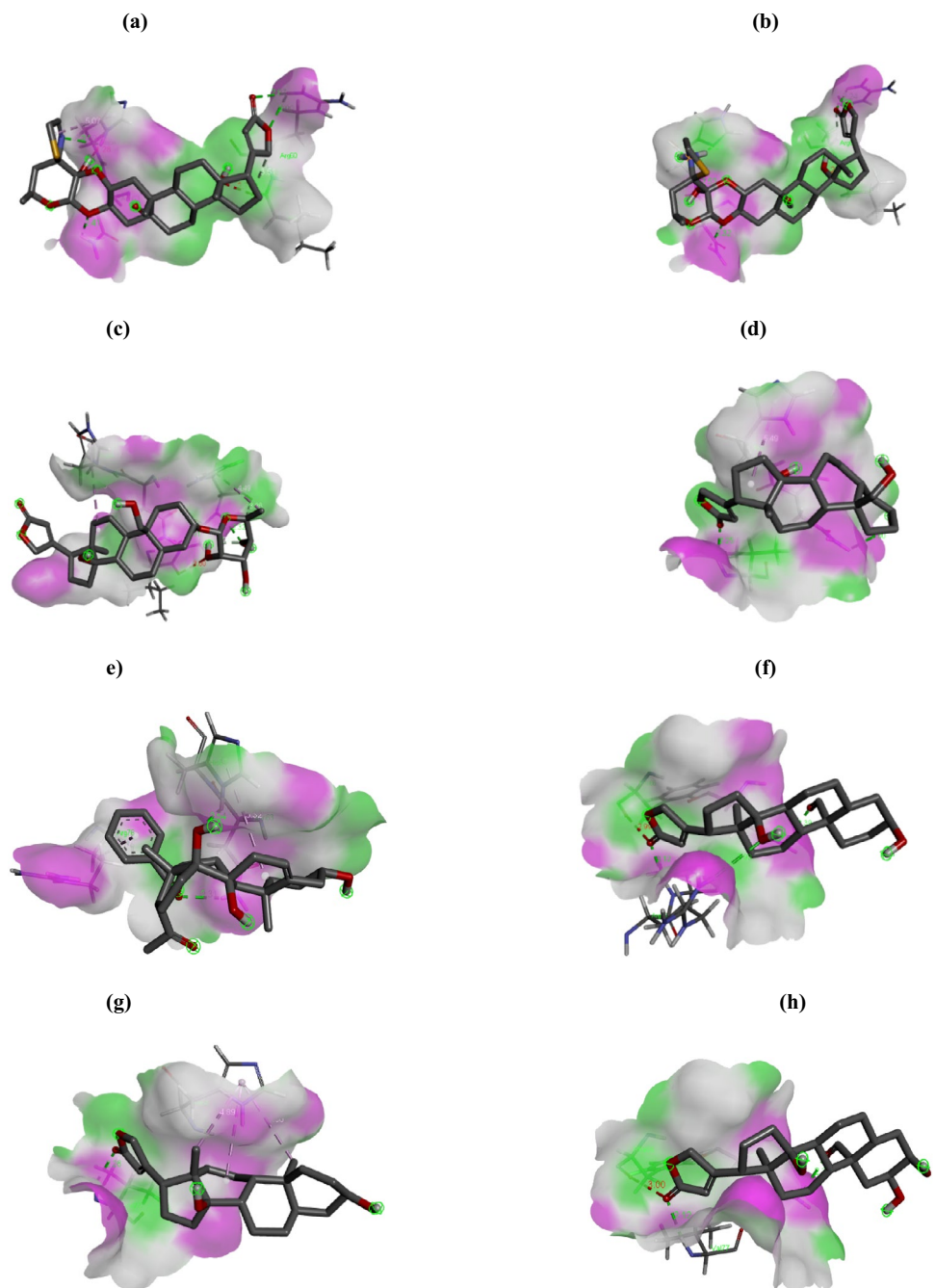
Density Functional Theory (DFT) Analysis

The best five ligand-receptor complexes were selected for DFT analysis. The band gap difference, *i.e.*, the differences between the E_{LUMO} and E_{HOMO} , ranged from 0.022 to 0.196 kcal/mol for the 5 selected phytochemicals. Comparing the band gaps among the selected phytochemicals, the most reactive potential phytochemical was identified against the target protein. Uscharin had the highest reactivity against SARS-CoV-2 main protease protein among the five phytochemicals, with a band energy gap of 0.022 kcal/mol. A summary of the DFT analysis is presented in Table 5.

Table 3 Functions of interacting human proteins with virus protein

Virus protein	Interacting human protein
3C like proteinase (3CLp)	CXCL10: Monocyte and T-lymphocyte chemotactic chemokine (C-X-C motif) ligand 10. connects to CXCR3
	EIF2C1: For RNA-mediated gene silencing (RNAi), eukaryotic translation initiation factor 2C is necessary. It inhibits the translation of mRNAs, such as microRNAs or small interfering RNAs, that are complementary to the short RNAs (siRNAs). Additionally necessary for the complementary promoter regions of bound short antigen RNAs to silence transcriptional genes (TGS) (agRNAs)
	EIF2C2: The RNA-induced silencing complex (RISC) requires the eukaryotic translation initiation factor 2C, 2 for RNA-mediated gene silencing (RNAi) (RISC). The "minimum RISC" seems to include AGO2, which is connected to a short guide RNA, either a short interfering RNA (siRNA) or microRNA (miRNA). These guide RNAs through RISC to mRNAs that are complementary to one other and are meant to be targets for silence. The level of complementarity between the target and the miRNA or siRNA determines the exact mechanism of gene silencing. Endon-mediated silencing is often the consequence of RISC binding to an mRNA that is completely complementary
	EIF2C3: For eukaryotic translation initiation factor 2C, RNA-mediated gene silencing and 3 is crucial (RNAi), the translation of mRNAs that are complementary to them is suppressed when it binds to tiny RNAs like microRNAs (miRNAs), has no endonuclease activity and doesn't seem to cleave target mRNAs, which may play a role in the stability of small RNA derivatives (riRNA) created from RNA polymerase III-transcribed RNA after processing. Alu repeats with a DR2 retinoic acid reply element degrade a subset of RNA polymerase II-transcribed genes later by riRNA in stem cells (RARE)
	EIF2C4: For RNA-mediated gene silencing, the eukaryotic translation initiation factor 2C, 4 is necessary (RNAi), suppresses the translation of short complementary mRNAs, such as microRNAs (miRNAs), by binding to them, does not seem to cleave target mRNAs and lacks endonuclease activity. Additionally necessary for the human hepatitis delta virus's RNA-directed transcription and replication (HDV)

Fig. 3 Interaction of **a** Ucharin **b** Voruscharin **c** Frugoside **d** Coroglaucogenin **e** Benzoyl-solineolone **f** Corotoxigenin **g** Uzarigenin **h** Calotropagenin **i** Isolineolone **j** Syriogenin **k** Lineolone **l** Benzoyl-lineolone **m** Melissyl-Alcohol **(n)** Beta-Sitosterol with the binding sites of main protease (3CLp) protein from SARS-CoV-2. H-bond donors are represented by the purple hue, and H-bond acceptors by the green color



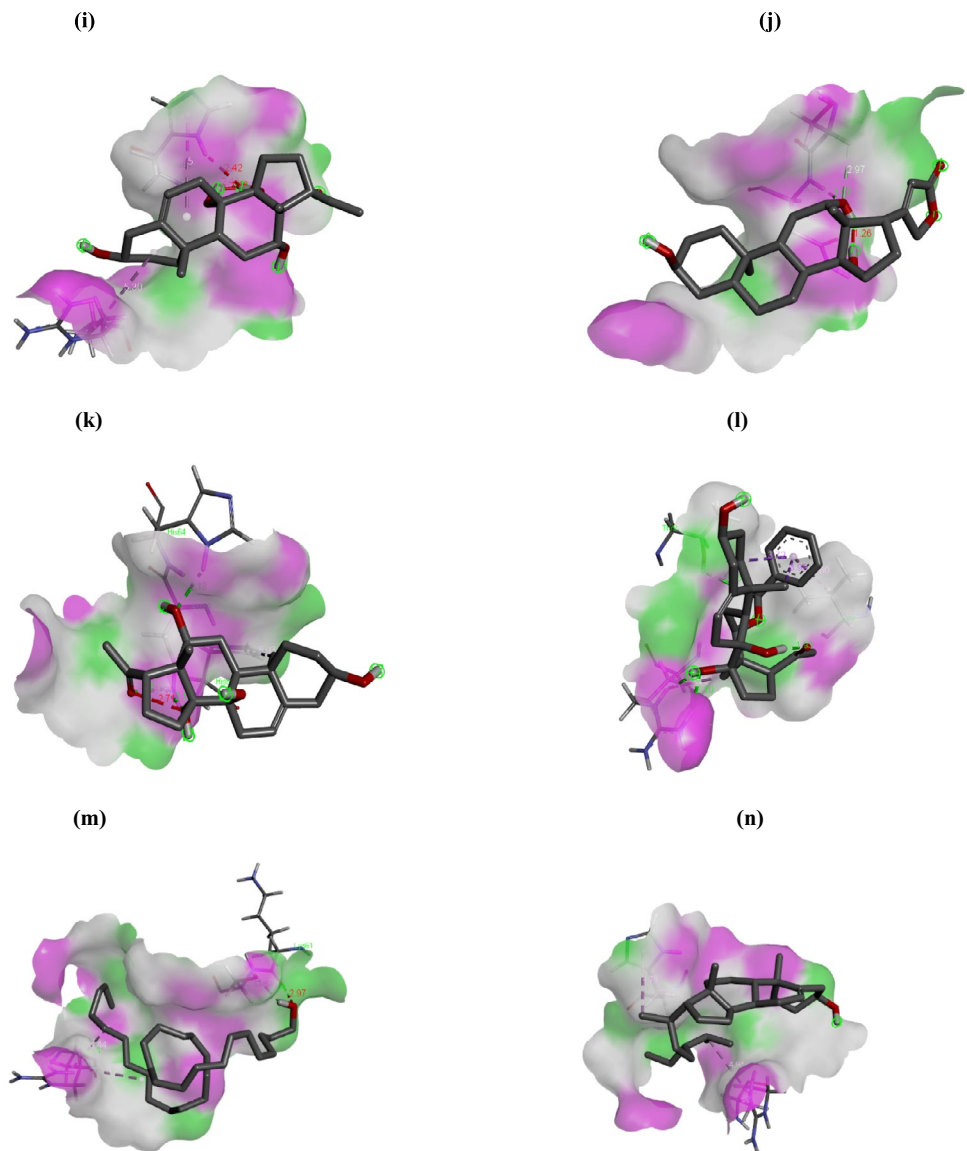
Other Considerations

Although important the delivery of the phytochemicals to the targeted sites like nanoparticles formulation [43, 44] is beyond the scope of this study. Also, the study lacks in vivo analysis.

Conclusion

The virus SARS-CoV-2 has drastically affected the global life. This study aims at targeting the virus using computer-assisted drug discovery. *Calotropis procera*

Fig. 3 (continued)



being important medicinal plant in context with the viral infection needs much emphasis. In the present study, out of 52 phytochemicals from *Calotropis procera*, 14 were screened having drug-like potential. The docking results revealed that 11 of the 14 phytochemicals had a high binding affinity for the main protease protein. Among all, the phytochemicals uscharin, voruscharin, frugoside, coroglaucigenin, and benzoylisolineolone may be considered the top 5 drug-like candidates against 3CLp. DFT analysis

of the best 5 phytochemicals revealed that the uscharin exhibited higher reactivity as the band energy gap was the least (0.022 kcal/mol) among the five selected candidates. These phytochemicals can further be investigated in vitro and in vivo for their effectiveness and safety as potential anti-SARS-CoV-2 drug candidates, specifically the MD simulation, cell line assays and animal models-based assays.

Table 4 Docking results of phytochemicals with SARS-CoV-2 main protease (3CLp) (PDB: 6XA4)

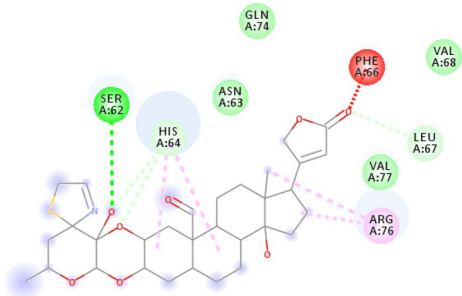
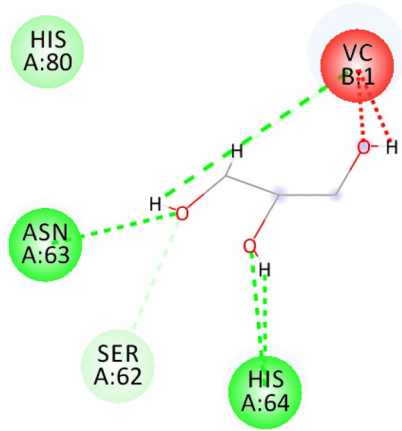
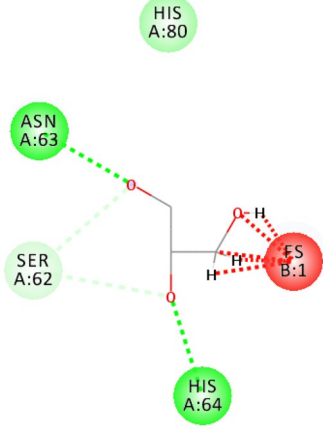
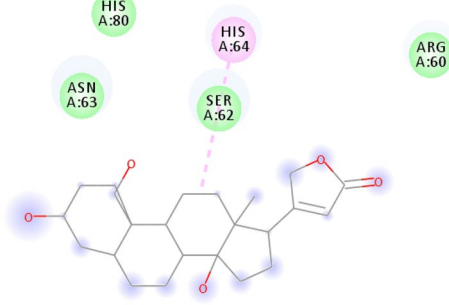
SN	Phytochemical	2D Figures (Interacting Residues)	Interacting Amino Acids	Binding Affinities (kcal/mol)	K _i (μM)	H-bonds
1	USCHARIN		His ₆₄ , Arg ₇₆ , Ile ₅₉ , Asn ₆₃ , Ser ₆₂ , Gln ₇₄ , Val ₇₇ , Leu ₆₇ ,	- 6.7	12.118	2
2	VORUSCHARIN		His ₆₄ , Asn ₆₃ , Arg ₆₀ , Ile ₅₉ , His ₈₀ , Ser ₆₂	- 6.5	16.989	2
3	FRUGOSIDE		His ₈₀ , His ₆₄ , Gly ₇₉ , Ile ₇₈ , Asn ₆₃ , Ser ₆₂	- 5.4	108.988	2
4	COROGLAUCOGENIN		His ₆₄ , Val ₇₇ , Asn ₆₃ , Ser ₆₂ , His ₈₀ , Arg ₆₀	- 5.6	77.735	1

Table 4 (continued)

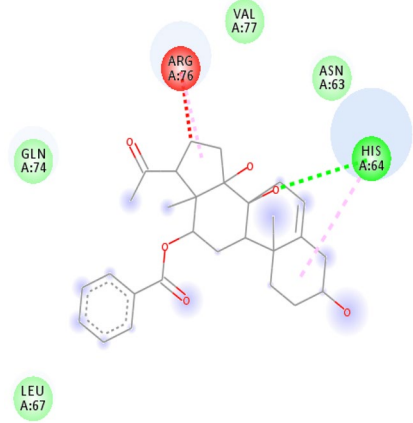
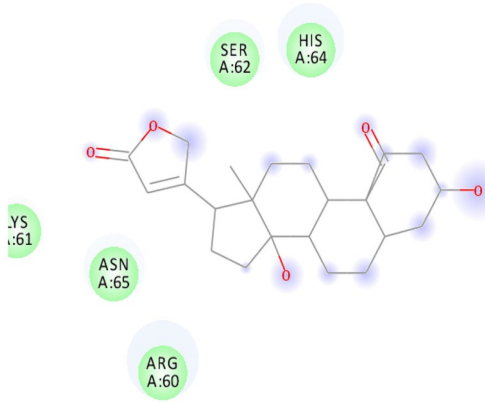
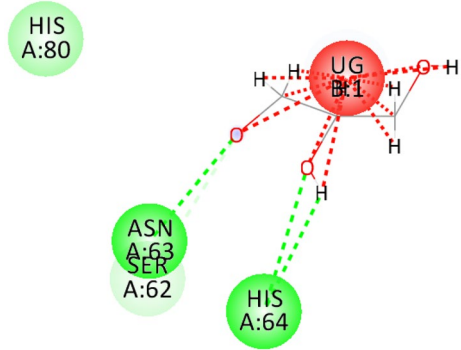
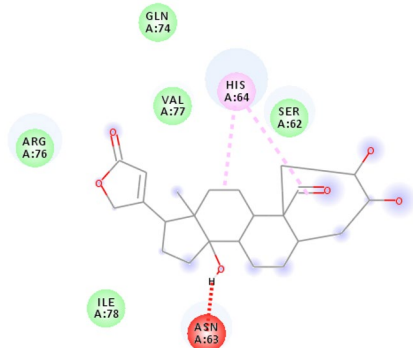
SN	Phytochemical	2D Figures (Interacting Residues)	Interacting Amino Acids	Binding Affinities (kcal/mol)	K _i (μM)	H-bonds
5	BENZOYLISOLINEOLONE		His ₆₄ , Asn ₆₃ , Arg ₇₆ , Val ₇₇ , Gln ₇₄ , Leu ₆₇	- 5.1	180.936	1
6	COROTOXIGENIN		Arg ₇₆ , Asn ₆₃ , Val ₇₇ , Phe ₆₆ , Ser ₆₂ , Asn ₆₅ , Arg ₆₀	- 4.9	253.681	2
7	UZARIGENIN		His ₆₄ , Val ₇₇ , Asn ₆₃ , Ser ₆₂ , His ₆₄	- 5.0	214.243	1
8	CALOTROPA-GENIN		Asn ₆₃ , Val ₇₇ , Phe ₆₆ , Gln ₇₄ , Arg ₇₆ , Ile ₇₈ , Ser ₆₂	- 4.8	300.379	2

Table 4 (continued)

SN	Phytochemical	2D Figures (Interacting Residues)	Interacting Amino Acids	Binding Affinities (kcal/mol)	K _i (μM)	H-bonds
9	ISOLINEOLONE		His ₆₄ , Arg ₇₆ , Gly ₂₃ , Cys ₂₂ , Lys ₆₁ , Arg ₆₀	- 4.9	253.681	1
10	SYRIOGENIN		Asn ₆₃ , Ser ₆₂ ,	- 4.8	300.379	1
11	LINEOLONE		His ₆₄ , His ₈₀ , Asn ₆₃ , Ser ₅₂ , Arg ₇₆ ,	- 4.4	590.470	2
12	BENZOYLLINEOLONE		Arg ₇₆ , Thr ₉₃ , Val ₇₃ , Asn ₆₃ , His ₆₄ , Arg ₆₀ , Leu ₅₈ , Ser ₆₂ , His ₈₀	- 4.0	1160.713	1

Table 4 (continued)

SN	Phytochemical	2D Figures (Interacting Residues)	Interacting Amino Acids	Binding Affinities (kcal/mol)	K _i (μM)	H-bonds
13	MELISSYL-ALCOHOL		Arg ₇₆ , Ser ₆₂ , Lys ₆₁ , Val ₇₇ , Asn ₆₃ , His ₈₀	- 2.8	8816.729	1
14	BETA-SITOSTEROL		His ₆₄ , Arg ₇₆ , Asn ₆₃ , Ser ₆₂ , His ₈₀	- 4.1	980.264	0

Table 5 Analysis of phytochemicals against the major protease protein of SARS-CoV-2 based on density functional theory

Phytochemicals	E _{HOMO} (Kcal/mol)	E _{LUMO} (Kcal/mol)	Band energy gap (ΔE) (Kcal/mol)
Ucharin	- 0.105	- 0.083	0.022
Voruscharin	- 0.236	- 0.055	0.181
Frugoside	- 0.260	- 0.050	0.21
Coroglaucogenin	- 0.108	- 0.070	0.038
Benzoylisolineolone	- 0.249	- 0.053	0.196

Supplementary Information The online version contains supplementary material available at <https://doi.org/10.1007/s12033-024-01253-z>.

Acknowledgements Researchers Supporting Project number (RSP2024R242), King Saud University, Riyadh, Saudi Arabia.

Author Contributions The manuscript was written with the contributions of all authors. All authors have approved the final version of the manuscript.

Funding This study was funded by King Saud University, RSP2024R242, Khalid M. Alotaibi.

Data Availability The datasets generated during and/or analyzed during the current study are available from the corresponding author upon reasonable request.

Declarations

Competing Interest The authors declare no conflict of interest.

References

- Lodish, H., & Zipursky, S. L. (2001). Molecular cell biology. *Biochemistry and Molecular Biology Education*, 29, 126–133.
- Hu, S., Jiang, S., Qi, X., Bai, R., Ye, X., & Xie, T. (2022). Races of small molecule clinical trials for the treatment of COVID-19: An up-to-date comprehensive review. *Drug Development Research*, 83(1), 16–54.
- Wang, M., Xie, Z., Xu, J., & Feng, Z. (2020). TWEAK/Fn14 axis in respiratory diseases. *Clinica Chimica Acta*, 509, 139–148.
- Lou, J., Zhao, L., Huang, Z., Chen, X., Xu, J., TAI, W. C., Tsim, K. W. K., Chen, Y.T., & Xie, T. (2021). Ginkgetin derived from Ginkgo biloba leaves enhances the therapeutic effect of cisplatin via ferroptosis-mediated disruption of the Nrf2/HO-1 axis in EGFR wild-type non-small-cell lung cancer. *Phytomedicine*, 80, 153370.
- Hu, F., Qiu, L., & Zhou, H. (2022). Medical device product innovation choices in Asia: An empirical analysis based on product space. *Frontiers in Public Health*, 10, 871575.
- Zhou, P., Yang, X. L., Wang, X. G., Hu, B., Zhang, L., Zhang, W., Si, H. R., Zhu, Y., Li, B., Huang, C. L., Chen, H. D., Chen, J., Luo, Y., Guo, H., Jiang, R. D., Liu, M. Q., Chen, Y., Shen, X. R., Wang, X., ... Shi, Z. L. (2020). A pneumonia outbreak associated with a new coronavirus of probable bat origin. *Nature*, 579, 270–273.
- Andersen, K. G., Rambaut, A., Lipkin, W. I., Holmes, E. C., & Garry, R. F. (2020). The proximal origin of SARS-CoV-2. *Nature Medicine*, 26(4), 450–452.
- Huang, C., Wang, Y., Li, X., Ren, L., Zhao, J., Hu, Y., Zhang, L., Fan, G., Xu, J., Gu, X., Cheng, Z., Yu, T., Xia, J., Wei, Y., Wu, W., Xie, X., Yin, W., Li, H., Liu, M., ... Cao, B. (2020). Clinical features of patients infected with 2019 novel coronavirus in Wuhan China. *The Lancet*, 395(10223), 497–506.

9. Bahadur, A., Saeed, A., Shoaib, M., Iqbal, S., & Anwer, S. (2019). Modulating the burst drug release effect of waterborne polyurethane matrix by modifying with polymethylmethacrylate. *Journal of Applied Polymer Science*, *136*, 47253.
10. Zhang, T., Wu, Q., & Zhang, Z. (2020). Probable pangolin origin of SARS-CoV-2 associated with the COVID-19 outbreak. *Current Biology*, *30*(7), 1346–1351.
11. Halaji, M., Farahani, A., Ranjbar, R., Heiat, M., & Dehkordi, F. S. (2020). Emerging coronaviruses: First SARS, second MERS and third SARS-CoV-2: Epidemiological updates of COVID-19. *Le Infezioni in Medicina*, *28*, 6–17.
12. Bahadur, A., Shoaib, M., Iqbal, S., Saeed, A., ur Rahman, M. S., & Channar, P. A. (2018). Regulating the anticancer drug release rate by controlling the composition of waterborne polyurethane. *Reactive and Functional Polymers*, *131*, 134–141.
13. Fehr, A. R., & Perlman, S. (2015). Coronaviruses: an overview of their replication and pathogenesis. *Coronaviruses* (pp. 1–23). Springer.
14. Khan, S., Iqbal, S., Khan, M., Rehman, W., Shah, M., Hussain, R., Rasheed, L., Khan, Y., Dera, A. A., Pashameah, R. A., Alzahrani, E., & Farouk, A. E. (2022). Design, synthesis, in silico testing, and in vitro evaluation of thiazolidinone-based benzothiazole derivatives as inhibitors of α -amylase and α -glucosidase. *Pharmaceuticals*, *15*, 1164.
15. Brian, D. A., & Baric, R. S. (2005). Coronavirus genome structure and replication. *Coronavirus replication and reverse genetics* (pp. 1–30). Springer.
16. Khan, S., Iqbal, S., Rehman, W., Hussain, N., Hussain, R., Shah, M., Ali, F., Fouda, A. M., Khan, Y., Dera, A. A., Alahmdi, M. I., Bahadur, A., Al-ghulikhah, H. A., & Elkaeed, E. B. (2023). Synthesis, molecular docking and ADMET studies of bis-benzimidazole-based thiadiazole derivatives as potent inhibitors, in vitro α -amylase and α -glucosidase. *Arabian Journal of Chemistry*, *16*, 104847.
17. Naqvi, A. A. T., Fatima, K., Mohammad, T., Fatima, U., Singh, I. K., Singh, A., Atif, S. M., Hariprasad, G., Hasan, G. M., & Hassan, M. I. (2020). Insights into SARS-CoV-2 genome, structure, evolution, pathogenesis and therapies: Structural genomics approach. *Biochimica et Biophysica Acta (BBA)—Molecular Basis of Disease*. <https://doi.org/10.1016/j.bbadis.2020.165878>
18. Liang, Y., Wang, M. L., Chien, C. S., Yarmishyn, A. A., Yang, Y. P., Lai, W. Y., Luo, Y. H., Lin, Y. T., Chen, Y. J., Chang, P. C., & Chiou, S. H. (2020). Highlight of immune pathogenic response and hematopathologic effect in SARS-CoV, MERS-CoV, and SARS-Cov-2 infection. *Frontiers in Immunology*, *11*, 1022.
19. Khan, S., Iqbal, S., Shah, M., Rehman, W., Hussain, R., Rasheed, L., Alrbyawi, H., Dera, A. A., Alahmdi, M. I., Pashameah, R. A., Alzahrani, E., & Farouk, A. E. (2022). Synthesis, in vitro anti-microbial analysis and molecular docking study of aliphatic hydrazide-based benzene sulphonamide derivatives as potent inhibitors of α -glucosidase and urease. *Molecules*, *27*, 7129.
20. Zhang, H., Penninger, J. M., Li, Y., Zhong, N., & Slutsky, A. S. (2020). Angiotensin-converting enzyme 2 (ACE2) as a SARS-CoV-2 receptor: Molecular mechanisms and potential therapeutic target. *Intensive care medicine*, *46*(4), 586–590.
21. Jeffers, S. A., Tusell, S. M., Gillim-Ross, L., Hemmila, E. M., Achenbach, J. E., Babcock, G. J., Thomas, W. D., Jr., Thackray, L. B., Young, M. D., Mason, R. J., Ambrosino, D. M., Wentworth, D. E., DeMartini, J. C., & Holmes, K. V. (2004). CD209L (L-SIGN) is a receptor for severe acute respiratory syndrome coronavirus. *Proceedings of the National Academy of Sciences*, *101*(44), 15748–15753.
22. Khan, S., Iqbal, S., Taha, M., Rahim, F., Shah, M., Ullah, H., Bahadur, A., Alrbyawi, H., Dera, A. A., Alahmdi, M. I., Pashameah, R. A., Alzahrani, E., & Farouk, A. E. (2022). Synthesis, in vitro biological evaluation and in silico molecular docking studies of indole based thiadiazole derivatives as dual inhibitor of acetylcholinesterase and butyrylcholinesterase. *Molecules*, *27*, 7368.
23. World Health Organization. (2019). *WHO global report on traditional and complementary medicine 2019*. World Health Organization.
24. Shoaib, M., Bahadur, A., ur Rahman, M. S., Iqbal, S., Arshad, M. I., Tahir, M. A., & Mahmood, T. (2017). Sustained drug delivery of doxorubicin as a function of pH, releasing media, and NCO contents in polyurethane urea elastomers. *Journal of Drug Delivery Science and Technology*, *39*, 277–282.
25. Zinatloo-Ajabshir, S., Morassaei, M. S., Amiri, O., Salavati-Niasari, M., & Foong, L. K. (2020). Nd₂Sn₂O₇ nanostructures: Green synthesis and characterization using date palm extract, a potential electrochemical hydrogen storage material. *Ceramics International*, *46*, 17186–17196.
26. Zinatloo-Ajabshir, S., Morassaei, M. S., & Salavati-Niasari, M. (2019). Eco-friendly synthesis of Nd₂Sn₂O₇-based nanostructure materials using grape juice as green fuel as photocatalyst for the degradation of erythrosine. *Composites Part B: Engineering*, *167*, 643–653.
27. Zinatloo-Ajabshir, S., & Salavati-Niasari, M. (2016). Facile route to synthesize zirconium dioxide (ZrO₂) nanostructures: Structural, optical and photocatalytic studies. *Journal of Molecular Liquids*, *216*, 545–551.
28. Zinatloo-Ajabshir, S., Mahmoudi-Moghaddam, H., Amiri, M., & Akbari Javar, H. (2024). A green and simple procedure to synthesize dysprosium cerate plate-like nanostructures and their application in the electrochemical sensing of mesalazine. *Journal of Materials Science: Materials in Electronics*. <https://doi.org/10.1007/s10854-024-12137-y>
29. Lipinski, C. A., Lombardo, F., Dominy, B. W., & Feeney, P. J. (1997). Experimental and computational approaches to estimate solubility and permeability in drug discovery and development settings. *Advanced Drug Delivery Reviews*, *23*(1–3), 3–25.
30. Laskowski, R. A., MacArthur, M. W., Moss, D. S., & Thornton, J. M. (1993). PROCHECK: A program to check the stereochemical quality of protein structures. *Journal of Applied Crystallography*, *26*(2), 283–291.
31. Garnier, J., Gibrat, J. F., & Robson, B. (1996). GOR method for predicting protein secondary structure from amino acid sequence. *Methods in Enzymology*, *266*, 540–553.
32. Von Mering, C., Jensen, L. J., Snel, B., Hooper, S. D., Krupp, M., Foglierini, M., Jouffre, N., Huynen, M. A., & Bork, P. (2005). STRING: known and predicted protein–protein associations, integrated and transferred across organisms. *Nucleic Acids Research*, *33*, 433–437.
33. Tarasova, O., Poroikov, V., & Veselovsky, A. (2018). Molecular docking studies of HIV-1 resistance to reverse transcriptase inhibitors: Mini-review. *Molecules*, *23*(5), 1233.
34. Thai, K. M., Le, D. P., Tran, T. D., & Le, M. T. (2015). Computational assay of Zanamivir binding affinity with original and mutant influenza neuraminidase 9 using molecular docking. *Journal of Theoretical Biology*, *385*, 31–39.
35. Gaussian 16, Revision C.01, M. J. Frisch, G. W. Trucks, H. B. Schlegel, G. E. Scuseria, M. A. Robb, Gaussian, Inc., Wallingford CT, 2016.
36. GaussView, Version 6.1, R. Dennington, T. A. Keith, and J. M. Millam, Semichem Inc., Shawnee Mission, KS, 2016.
37. Gill, P. M., Johnson, B. G., Pople, J. A., & Frisch, M. J. (1992). The performance of the Becke–Lee–Yang–Parr (B–LYP) density functional theory with various basis sets. *Chemical Physics Letters*, *197*, 499–505.

38. Benet, L. Z., Hosey, C. M., Ursu, O., & Oprea, T. I. (2016). BDDCS, the rule of 5 and drugability. *Advanced Drug Delivery Reviews*, *101*, 89–98.
39. Qaddir, I., Rasool, N., Hussain, W., & Mahmood, S. (2017). Computer-aided analysis of phytochemicals as potential dengue virus inhibitors based on molecular docking, ADMET and DFT studies. *Journal of Vector Borne Diseases*, *54*(3), 255.
40. Hoof, R. W., Sander, C., & Vriend, G. (1997). Objectively judging the quality of a protein structure from a Ramachandran plot. *Bioinformatics*, *13*(4), 425–430.
41. Kabsch, W., & Sander, C. (1983). Dictionary of protein secondary structure: pattern recognition of hydrogen-bonded and geometrical features. *Biopolymers: Original Research on Biomolecules*, *22*(12), 2577–2637.
42. Zhu, W., Xu, M., Chen, C. Z., Guo, H., Shen, M., Hu, X., Shinn, P., Klumpp-Thomas, C., Michael, S. G., & Zheng, W. (2020). Identification of SARS-CoV-2 3CL protease inhibitors by a quantitative high-throughput screening. *ACS Pharmacology & Translational Science*, *3*(5), 1008–1016. <https://doi.org/10.1021/acscptsci.0c00108>
43. Zinatloo-Ajabshir, Z., & Zinatloo-Ajabshir, S. (2019). Preparation and characterization of curcumin niosomal nanoparticles via a simple and eco-friendly route. *Journal of Nanostructures*, *9*(4), 784–790.
44. Qazvini, N. T., & Zinatloo, S. (2011). Synthesis and characterization of gelatin nanoparticles using CDI/NHS as a non-toxic cross-linking system. *Journal of Material Science Material in Medicine*, *22*(1), 63–69. <https://doi.org/10.1007/s10856-010-4178-2>

Publisher's Note Springer Nature remains neutral with regard to jurisdictional claims in published maps and institutional affiliations.

Springer Nature or its licensor (e.g. a society or other partner) holds exclusive rights to this article under a publishing agreement with the author(s) or other rightsholder(s); author self-archiving of the accepted manuscript version of this article is solely governed by the terms of such publishing agreement and applicable law.